Ammonia−Water Cation and Ammonia Dimer Cation

Hahn Kim

Pohang Jecheol High School, Pohang 790-390, Korea

Han Myoung Lee*

Center for Basic Sciences, Department of Chemistry, Pohang University of Science and Technology, Pohang 790-784, Korea

Received: April 3, 2009; Revised Manuscript Received: May 7, 2009

We have investigated the structure, interaction energy, electronic properties, and IR spectra of the ammonia−water cation $(NH_3H_2O)^+$ using density functional theory (DFT) and high-level ab initio theory. The ammonia−water cation has three minimum-energy structures of (a) $H_2NH^+\cdots OH_2$, (b) $H_3N^+\cdots OH_2$, and (c) $H_3NH^+\cdots OH$. The lowest-energy structure is (a), followed by (c) and (b). The ammonia dimer cation has two minimum-energy structures [the lowest $H_3NH^+\cdots NH_2$ structure and the second lowest $(H_3N\cdots NH_3)^+$ structure]. The minimum transition barrier for the interconversion between (a), (b), and (c) is ∼6 kcal/mol. Most DFT calculations with various functionals, except a few cases, overstabilize the N···O and N···N binding, predicting different structures from Möller−Plesset second-order perturbation (MP2) theory and the most reliable complete basis set (CBS) limit of coupled cluster theory with single, double, and perturbative triple excitations [CCSD(T)]. Thus, the validity test of the DFT functionals for these ionized molecular systems would be of importance.

Introduction

Extensive studies of dissociation of acids, bases, and salts have been carried out to understand solvation phenomena.[1−3] These phenomena are strongly involved in H-bonding and proton transfer. For a better understanding of H-bonding and proton transfer, it would be of interest to investigate such phenomena in the ionized state, which can be easily observable in the stratosphere. We are particularly interested in the hydration of the ammonia cation, namely, $(NH_3\cdots H_2O)^+$.

Ammoinum cluster cations $(NH_3)_n^+$ and their hydrated clusters $[(NH_3)_n[(H_2O)_m]^+$ were experimentally produced under special conditions in the gas phase.[4] A few theoretical investigations for ammonia, water, and ammonia−water cluster cations were performed.[5−8] The ammonia dimer cation and the ammonia−water cation were experimentally discussed.[9] For the ammonia dimer cation, the disproportionated ionic structure $(NH_4^+\cdots NH_2)$ was predicted to be more stable than the hydrazine-like structure $(H_3N\cdots NH_3)$.[6] In previous work, one of us reported that for the water dimer cation at high levels of ab initio theory, the $H_3O^+\cdots OH$ structure is much more stable than the $H_2O\cdots OH_2$ structure.[10]

Here, we investigate the structures, energetics, and spectra of the ammonia−water cation $(NH_3H_2O)^+$ and the ammonia dimer cation $(NH_3)_2^+$ using high levels of ab initio theory. We compare the DFT, MP2, and CCSD(T) results. Serious failures for most DFT calculations are found, except for few functionals.

Calculation Methods

Before calculating the ionized structure of the ammonia−water cluster and the ammonia dimer, we need to calculate their neutral structure as the reference system. Since these structures are already well-known,[11,12] we calculated their structures and energies at the CCSD(T)/aVQZ//CCSD(T)/aVDZ level of theory. For the ionized structures, various structures of the ammonia−water cation and the ammonia dimer cation are optimized by using DFT methods with various functionals.

For the DFT calculations, we employ various functionals, Becke's exchange and Lee−Yang−Parr correlation functionals (BLYP),[13] Becke's exchange and Perdew−Wang correlation functionals (BPW91),[14] Handy's family functional including gradient-corrected correlation (HCTH407),[15] the local spin density approximation, Vosko−Wilk−Nusair correlation and Slater exchange functionals (LSDA: SVWN),[16] semiempirical-correction to BLYP for dispersion (BLYP-D),[17] Tao−Perdew−Staroverov−Scuseria exchange and τ-dependent gradient-corrected functionals (TPSS),[18] Becke's three-parameters for exchange and Lee−Yang−Parr correlation functionals (B3LYP),[19] Zhao and Truhlar's parametrized exchange and correlation hybrid meta-GGA M05-2X,[20] Perdew−Burke−Ernzerhof hybrid functional (PBE1PBE),[21] modified Perdew−Wang one-parameter model/modified Perdew−Wang and Becke one-parameter model for kinetics (MPW1K/MPWB1K),[22,23] Becke's half HF-LSDA (Hartree−Fock Local Spin Density Approximation) exchange and Lee−Yang−Parr correlation functionals (BH&H),[24] and Becke's half HF-LSDA-Becke exchange and Lee−Yang−Parr correlation functionals (BH&HLYP).[25] For these DFT calculations, we used the 6-311++G** basis set.[26] Then, as noted in the water dimer cation,[10] we also find that in the ammonia−water cation and the ammonia dimer cation, DFT/MPW1K and DFT/ BH&HLYP are reliable, while others give seriously wrong energy values, as compared with the CCSD(T)/CBS values. Here, we compare the DFT, MP2, and CCSD(T) results using the aug-cc-pVDZ, aug-cc-pVTZ, and aug-cc-pVQZ basis sets[27] (which will be denoted as aVDZ, aVTZ, and aVQZ, respectively). The CBS limit interaction energies were obtained with the extrapolation

* To whom correspondence should be addressed. E-mail: abcd0lhm@postech.ac.kr.

10.1021/jp903093a CCC: $40.75 © 2009 American Chemical Society
Published on Web 06/02/2009

(a) NH_3H_2O (b) $(NH_3)_2$

Figure 1. Structures for the neutral states of the ammonia−water cluster and the ammonia dimer at the CCSD(T)/aVDZ level of theory.

TABLE 1: Vertical/Adiabatic Ionization Energies (IP_v/IP_a in eV) and Protonation/Deprotonation Energies (E_{prot}/E_{deprot} in kcal/mol) of NH_3, H_2O, NH_3H_2O, and $(NH_3)_2$ at the CCSD(T)/aVQZ//CCSD(T)/aVDZ Level

	IP_v	IP_a	E_{prot}	E_{deprot}
NH_3	10.97	10.19	−9.19	17.92
H_2O	12.71	12.64	−7.44	17.23
NH_3H_2O	11.51	9.43	−9.79	16.83
$(NH_3)_2$	10.21	8.56	−10.19	17.42

scheme utilizing the fact that the electron correlation error is proportional to N^{-3} for the aug-cc-pV*N*Z basis set ($N = 2$: D; $N = 3$: T; $N = 4$: Q) [$\Delta E_{CBS} = (\Delta E_N N^3 - \Delta E_{N-1}(N-1)^3)/(N^3 - (N-1)^3)$].[28] Here, the CBS energies, which would give the most reliable values in these calculations, were obtained based on the aVTZ and aVQZ results. In this way, we could compare their CBS values and find the inherent errors in the DFT and MP2 results.

For the DFT and MP2 calculations using the aVDZ and aVTZ basis sets and the CCSD(T) calculations using the aVDZ basis set, the geometries were fully optimized, and frequency calculations were also carried out. A larger grid size (99, 974) than the ultrafine grid (99, 590) was employed to eliminate the imaginary frequencies for the DFT calculations. All of the optimizations were done by minimizing the total energy without any symmetry constraints. In the DFT and MP2 calculations using the aVQZ basis set, the corresponding aVTZ geometries were used, and the aVTZ frequencies were employed to obtain the zero-point energies (ZPEs) and thermal energies, while in the CCSD(T) calculations using the aVTZ and aVQZ basis sets, the corresponding aVDZ geometries were used, and the aVDZ frequencies were employed to obtain the ZPEs and thermal energies. For the basis set, the 1s orbitals of oxygen atoms were frozen in the correlation calculations. All of the "d" and "f" orbitals used here are the spherical harmonic basis functions (5d and 7f).

For the ionic structure, the basis set superposition energy (BSSE) correction can be made. However, in the nonionic structure, the positive charge is almost equally distributed in two monomer species so that the BSSE correction cannot be made properly. In order to compare the two structures at equal conditions, it is better not to make the BSSE corrections. Thus, the BSSE corrections are not considered in this system.

We calculated the ZPE's uncorrected total energy (ΔE_e) at the equilibrium states of the Born−Oppenheimer potential surfaces and the ZPE-corrected total energy (ΔE_0). The enthalpy/free-energy changes ($\Delta H_r/\Delta G_r$) at room temperature and 1 atm were obtained using the frequency calculations.

All of the calculations were carried out by using the Gaussian 03 suite of programs.[29] The BLYP-D calculations were done by using ORCA program[30] and the M05-2X calculations by Q-Chem program.[31] The molecular structures were drawn using the POSMOL package.[32]

Results and Discussion

Figure 1 shows the optimized neutral state structures of the ammonia−water cluster and the ammonia dimer at the CCSD(T)/aVDZ level. We calculated the vertical/adiabatic ionization energies (IP_v/IP_a) and protonation/deprotonation energies (E_{prot}/E_{deprot}) of NH_3 and H_2O at the CCSD(T)/aVQZ//CCSD(T)/aVDZ level (Table 1). For the ammonia monomer, the vertical/adiabatic IP (IP_v/IP_a) is 10.97/10.19 eV at the CCSD(T)/aVQZ//CCSD(T)/aVDZ level. These values are close to the experimental IP_v/IP_a (10.93/10.17 eV).[33] The N−H distance and HNH bond angle of the ammonia monomer cation are 1.031 Å and 120.0° at the CCSD(T)/aVDZ level, which shows 0.007 Å longer N−H distances and 14.1° wider bond angles than those of the neutral ammonia monomer (1.024 Å and 105.9° at the CCSD(T)/aVDZ level). The N−H bond strength becomes weaker, and the H−H repulsion is greater due to the ionization. Similarly, in case of the water monomer cation, the O−H distance and HOH bond

TABLE 2: DFT/6-311++G Interaction Energies[a] (kcal/mol) for Various Structures of the Ammonia−Water Cation $(NH_3H_2O)^+$ and the Ammonia Dimer Cation $(NH_3)_2^+$**

	$(NH3\cdots H2O)^+$			$(NH3\cdots NH3)^+$	
	$H_2NH^+\cdots OH_2$	$H_3N^+\cdots OH_2$	$H_3NH^+\cdots OH$	$H_3NH^+\cdots NH_2$	$(H_3N\cdots NH_3)^+$
method	$-\Delta E_e$ ($-\Delta E_0$)	$-\Delta E_e$ ($-\Delta E_0$)	$-\Delta E_e$ ($-\Delta E_0$)	$-\Delta E_e$ ($-\Delta E_0$)	$-\Delta E_e$ ($-\Delta E_0$)
BLYP	27.3(25.5)	**28.4**(25.3)	22.9(19.2)	42.8(40.0)	**47.6**(44.0)
BPW91	26.7(25.0)	**27.3**(24.0)	22.3(18.6)	43.0(40.3)	**46.7**(43.0)
HCTH407	26.0(24.2)	**26.8**(23.6)	22.0(18.2)	42.1(39.2)	**46.1**(42.4)
LSDA	35.8(34.2)	**37.9**(34.2)	26.2(22.7)	50.6*(48.0)*	**58.5**(54.7)
BLYP-D	27.8(26.3)	**29.8**(26.6)	23.5(19.4)	43.9(40.9)	**49.4**(45.6)
TPSS	**26.9**(25.1)	26.6(23.4)	23.7(19.9)	43.3(40.4)	**45.3**(41.6)
B3LYP	**26.3**(24.5)	24.1(20.8)	24.1(20.9)	42.8(39.7)	**43.6**(39.7)
M05−2X	**26.3**(24.1)	24.1(20.6)	25.1(19.9)	**42.4**(38.9)	41.4(37.8)
PBE1PBE	**27.1**(25.3)	23.3(20.1)	24.6(20.9)	**43.7**(40.7)	42.8(38.9)
BH&H	**31.5**(29.6)	25.4(22.6)	27.8(24.1)	**46.7**(43.6)	44.5(40.2)
BH&HLYP	**26.1**(24.0)	20.2(17.9)	25.7(22.0)	**42.2**(38.8)	37.0(32.9)
MPWB1K	**26.0**(24.1)	21.4(18.7)	25.2(21.4)	**42.5***(39.2)*	40.4(36.3)
MPW1K	**26.4**(24.5)	20.2(17.8)	24.9(21.1)	**42.8***(39.6)*	38.3(34.2)
CCSD(T)[b]	**24.1**(22.3)	18.2(16.0)	21.4(17.7)	**40.6**(37.5)	35.7(31.9)

[a] The interaction energy between one neutral ammonia/water monomer and one ammonia monomer cation is reported. ΔE_e are the ZPE-uncorrected energies at the equilibrium point of the Born−Oppenheimer potential surfaces, and ΔE_0 are the ZPE-corrected energies. The minimum-energy structures in ΔE_e are denoted in bold. The italic interaction energies in ($-\Delta E_0$) indicate that the calculated structure, although minimum, shows one imaginary frequency possibly due to the numerical instability. [b] CCSD(T)/CBS results.

TABLE 3: DFT, MP2, and CCSD(T) Interaction Energies (kcal/mol) of the Three Minimum-Energy Structures of the Ammonia−Water Cation $[(NH_3H_2O)^+]$[a]

	$H_2NH^+\cdots OH_2$				$H_3N^+\cdots OH_2$				$H_3NH^+\cdots OH$			
method	$-\Delta E_e$	$-\Delta E_0$	$-\Delta H_r$	$-\Delta G_r$	$-\Delta E_e$	$-\Delta E_0$	$-\Delta H_r$	$-\Delta G_r$	$-\Delta E_e$	$-\Delta E_0$	$-\Delta H_r$	$-\Delta G_r$
MPW1K/6-311++G**	26.43	24.45	25.36	17.43	20.18	17.78	18.36	11.08	24.92	21.10	21.86	14.49
MPW1K/aVTZ	24.97	23.25	24.05	16.39	18.70	16.06	16.77	9.30	23.76	20.01	20.78	13.99
MPW1K/aVQZ//	25.06	23.34	24.14	16.48	18.55	15.91	16.62	9.15	23.80	20.05	20.81	14.03
MPW1K/CBS	25.13	23.41	24.21	16.55	18.44	15.80	16.51	9.04	23.82	20.08	20.84	14.06
MP2/aVTZ	24.15	22.39	23.10	15.63	17.43	15.54	15.82	9.59	19.50	15.71	16.47	9.21
MP2/aVQZ//	24.19	22.42	23.14	15.66	17.49	15.60	15.88	9.65	19.14	15.35	16.11	8.84
MP2/CBS	24.21	22.45	23.16	15.69	17.54	15.65	15.92	9.70	18.87	15.09	15.84	8.58
CCSD(T)/aVTZ//	24.08	22.22	22.86	15.68	18.11	15.89	16.37	9.42	22.08	18.39	19.11	12.24
CCSD(T)/aVQZ//	24.11	22.25	22.90	15.71	18.18	15.96	16.43	9.49	21.66	17.97	18.70	11.82
CCSD(T)/CBS	24.14	22.27	22.92	15.73	18.23	16.01	16.48	9.54	21.36	17.67	18.39	11.52

[a] At the MPW1K and MP2 levels, "aVQZ//" denotes the calculations done at the aVTZ geometry along with the aVTZ ZPE and thermal energy corrections. At the CCSD(T) level, "aVTZ//" and "aVQZ//" denote the calculations done at the aVDZ geometry along with the aVDZ ZPE and thermal energy corrections.

TABLE 4: DFT, MP2, and CCSD(T) Interaction Energies (kcal/mol) for the Two Minimum-Energy Structures of the Ammonia Dimer Cation $[(NH_3)_2^+]$[a]

	$H_3NH^+\cdots NH_2$				$(H_3N\cdots NH_3)^+$			
method	$-\Delta E_e$	$-\Delta E_0$	$-\Delta H_r$	$-\Delta G_r$	$-\Delta E_e$	$-\Delta E_0$	$-\Delta H_r$	$-\Delta G_r$
MPW1K/6-311++G**	42.77				38.33	34.21	35.30	26.94
MPW1K/aVTZ	41.57				37.08	32.98	34.06	25.60
MPW1K/aVQZ//	41.63				37.23	33.13	34.21	25.75
MPW1K/CBS	41.68				37.34	33.24	34.32	25.85
MP2/aVTZ	40.23	37.15	38.01	30.70	35.64	31.26	32.41	23.43
MP2/aVQZ//	40.16	37.07	37.94	30.62	35.79	31.40	32.55	23.57
MP2/CBS	40.10	37.02	37.88	30.57	35.89	31.51	32.66	23.68
CCSD(T)/aVTZ//	40.81	37.68	38.53	30.87	35.42	31.60	32.68	23.70
CCSD(T)/aVQZ//	40.71	37.58	38.43	30.77	35.57	31.75	32.83	23.85
CCSD(T)/CBS	40.64	37.51	38.36	30.70	35.68	31.86	32.94	23.96

[a] At the MPW1K and MP2 levels, "aVQZ//" denotes the calculations done at the aVTZ geometry along with the aVTZ ZPE and thermal energy corrections. At the CCSD(T) level, "aVTZ//" and "aVQZ//" denote the calculations done at the aVDZ geometry along with the aVDZ ZPE and thermal energy corrections. The MPW1K thermal energies for $H_3NH^+\cdots OH$ are not reported due to imaginary frequencies, which were raised due possibly to the numerical instability.

angle (1.002 Å and 109.1°) are 0.04 Å longer and 4.9° wider than those of the neutral water monomer (0.962 Å and 104.2°) at the CCSD(T)/aVTZ level.

Figure 2 shows the DFT/MPW1K optimized structures of the ammonia−water cation and the ammonia dimer cation. For the ammonia−water cation, the minimum-energy structures are (a) $H_2NH^+\cdots OH_2$, (b) $H_3N^+\cdots OH_2$, and (c) $H_3NH^+\cdots OH$, and the transition-state (TS) structures between (a) and (c) and between (b) and (c) are (d) [TS]/ab and (e) [TS]/bc, respectively. For the ammonia dimer cation, the minimum-energy structures are (f) $H_3NH^+\cdots NH_2$ and (g) $(H_3N\cdots NH_3)^+$, and the TS between the two structures is (h) [TS]/fg. These structures and energetics are found to be similar to those obtained at the CCSD(T)/CBS//CCSD(T)/ aVDZ level, which will be discussed later.

We calculated the interaction energies for the dimerization between ammonia/water molecules, where the geometries for ammonia/water monomers were fully optimized in the dimer. For the ammonia−water cation, we may have two options for the interaction energies, $\Delta E_{NH_4^+} = E(\text{dimer cation}) - E(H_2O) - E(NH_3^+)$ or $\Delta E_{H_3O^+} = E(\text{dimer cation}) - E(H_2O^+) - E(NH_3)$. Since the protonation energy of NH_3 is smaller than that of H_2O, we report the interaction energy ΔE with $\Delta E_{NH_4^+}$. For the ammonia dimer cation, $\Delta E = E(\text{dimer cation}) - E(NH_3) - E(NH_3^+)$.

In the case of $(NH_3)_2^+$ (Table 2), the BLYP, BPW91, HCTH407, LSDA, BLYP-D, and TPSS calculations predict that

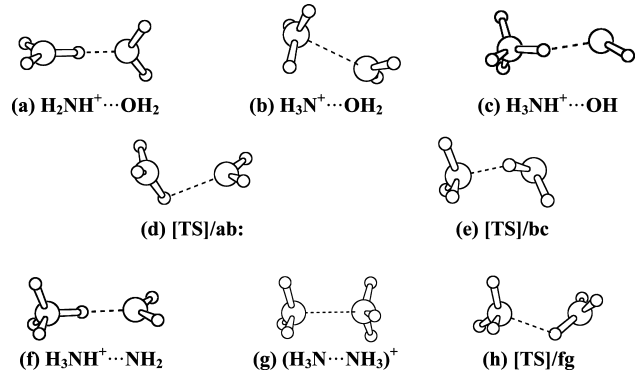

Figure 2. Minimum-energy and transition-state (TS) structures of the ammonia−water cation $[(NH_3H_2O)^+]$ (a−e) and ammonia dimer cation $[(NH_3)_2^+]$ (f−h). Notation "[TS]/ab" denotes the transition state between two minimum-energy structures (a) and (b). The minimum-energy structures are optimized at the CCSD(T)/aVDZ level, and the TS structures are optimized at the DFT/MPW1K level. The DFT/MPW1K structures and energies are similar to those at the CCSD(T)/aVQZ// CCSD(T)/aVDZ level.

the $(H_3N\cdots NH_3)^+$ structure is much more stable than the $H_3NH^+\cdots NH_2$ structure. The B3LYP, M05-2X, PBE1PBE, BH&H, and MPWB1K calculations predict that the two structures are compatible. On the other hand, the MPW1K and BH&HLYP calculations predict that the $H_3NH^+\cdots NH_2$ structure

TABLE 5: Geometrical Parameters [Distances (r/Å)] of the Ammonia−Water Cluster $(NH_3H_2O)^+$ and the Ammonia Dimer Cation $[(NH_3)_2^+]$[a]

	$H_2NH^+\cdots OH_2$					$H_3N^+\cdots OH_2$			$H_3NH^+\cdots OH$			
method	r_{N-O}	$r_{H\cdots O}$	r_{N-H+}	r_{N-H}	r_{O-H}	r_{N-O}	r_{N-H}	r_{O-H}	r_{N-O}	r_{N-H+}	r_{N-H}	r_{O-H}
MPW1K/aVTZ	2.575	1.495	1.080	1.013	0.954	2.282	1.008	0.956	2.781	1.037	1.014	0.967
MP2/aVTZ	2.611	1.540	1.071	1.017	0.965	2.380	1.015	0.965	2.808	1.040	1.020	0.973
CCSD(T)/aVDZ	2.631	1.553	1.078	1.028	0.968	2.348	1.025	0.970	2.832	1.046	1.028	0.981

	$H_3NH^+\cdots NH_2$				$(H_3N\cdots NH_3)^+$		NH_3	H_2O
method	r_{N-N}	$r_{H\cdots N}$	r_{N-H^+}	r_{N-H}	r_{N-N}	r_{N-H}	r_{N-H}	r_{O-H}
MPW1K/aVTZ	2.739	1.665	1.074	1.014	2.197	1.005	1.005	0.951
MP2/aVTZ	2.768	1.695	1.073	1.019	2.164	1.013	1.012	0.961
CCSD(T)/aVDZ	2.794	1.719	1.075	1.029	2.198	1.022	1.024	0.967

[a] The r_{N-H} and r_{O-H} report the average value for the non-hydrogen-bonded N−H and O−H distances, respectively. The data for the ammonia monomer and the water monomer are listed for comparison.

TABLE 6: MP2/aVQZ//MP2/aVTZ NBO Charges (q) of the Ammonia−Water Cation $(NH_3H_2O)^+$ and the Ammonia Dimer Cation $(NH_3NH_3)^+$

structure	$H_2NH^+\cdots OH_2$	$H_3N^+\cdots OH_2$	$H_3NH^+\cdots OH$	$H_3NH^+\cdots NH_2$	$(H_3N\cdots NH_3)^+$
moiety	NH_3	NH_3	NH_4	NH_4	NH_3
q(NBO)	0.909	0.956	0.948	0.885	0.500

is much more stable than the $(H_3N\cdots NH_3)^+$ structure. For these various DFT functionals, a similar trend is also noted in the case of $(NH_3\cdots H_2O)^+$ (Table 2). Let us denote L/L′ as a ligand representing NH_3 or OH_2 and denote L_d/L_d′ as a deprotonated ligand representing NH_2 or OH. Then, the L···L′ structure is favored over the $LH^+\cdots L_d$′ structure for BLYP, BPW91, HCTH407, LSDA, BLYP-D, and TPSS; the L···L′ structure is compatible with the $LH^+\cdots L_d$′ structure for B3LYP, M05-2X, and PBE1PBE, despite that the $LH^+\cdots L_d$′ structure is more favored over the L···L′ structure. Furthermore, L···L′ structure is the most stable for BLYP, BPW91, HCTH407, LSDA, and BLYP-D, while the $L_dH^+\cdots$L′ structure is the most stable for the other functionals. We find that MPW1K and BH&HLYP results are the most consistent with the CCSD(T) results, while the MPW1K results are slightly better than BH&HLYP, which will be discussed later. Thus, we report the detailed computational results of DFT/MPW1K, MP2, and CCSD(T) using the aVNZ basis sets (N = D/T/Q) and their CBS limit values (Table 3 and 4). In Table 3, according to CCSD(T)/CBS values, the lowest-energy structure of $(NH_3H_2O)^+$ is $H_2NH^+\cdots OH_2$, followed by $H_3NH^+\cdots$OH, and followed by $H_3N^+\cdots OH_2$. In Table 4, the lowest-energy structure of the ammonia dimer cation is $H_3NH^+\cdots NH_2$, followed by the $(H_3N\cdots NH_3)^+$.

The ammonia molecule is more easily ionized than the water molecule. On the unrestricted open-shell approach of the ammonia−water cluster, the calculated IP_v/IP_a of the lowest-energy structure $H_2NH^+\cdots OH_2$ is 11.51/9.43 eV at the CCSD(T)/aVQZ// CCSD(T)/ aVDZ level. The calculated IP_v/IP_a of the ammonia dimer is 10.21/8.56 eV at the CCSD(T)/aVQZ// CCSD(T)/aVDZ level. The calculated IP_v, IP_a, protonation energy (negative value of the proton affinity), and deprotonation energies are listed in Table 1.

Table 5 lists the optimized geometrical parameters of the structures at the MPW1K and MP2 levels for the aVTZ basis set and those at the CCSD(T) level for the aVDZ basis set. The N−H^+ distance (r_{N-H^+}) of the $H_2NH^+\cdots OH_2$ structure is longer than those of other ammonia−water cation structures. The N−H distance (r_{N-H}) of the $L_dH^+\cdots$L′ structure is longer than that of the L···L structure, expectedly. Table 6 shows the natural bond orbital (NBO) charges of the ammonia or ammonium fragments in the ammonia−water cation and the ammonia dimer cation at the MP2/aVQZ//MP2/aVTZ level. Since the ammonia

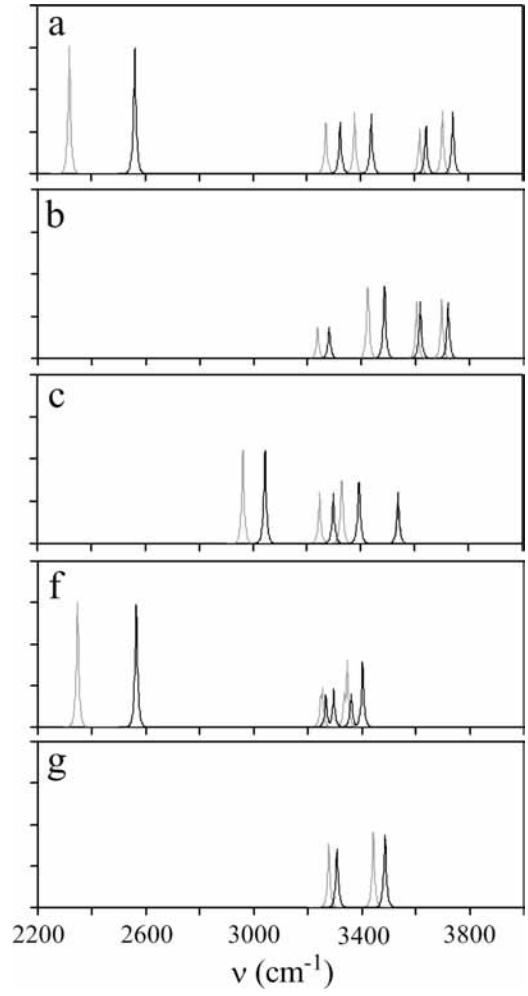

Figure 3. MPW1K/6-311++G** (gray) and CCSD(T)/aVDZ (black) predicted IR spectra for the N−H and O−H stretching frequencies of the ammonia−water cation [(a) $H_2NH^+\cdots OH_2$; (b) $H_3N^+\cdots OH_2$; (c) $H_3NH^+\cdots$OH] and ammonia dimer cation [(f) $H_3NH^+\cdots NH_2$; (g) $(H_3N\cdots NH_3)^+$]. For the CCSD(T) frequencies, the intensities are not available; therefore, the corresponding MPW1K intensities are employed.

TABLE 7: Scaled Frequencies [ν(cm^{-1})] and the IR Intensities (in 10 km/mol in subscripts) of NH and OH Stretching Modes for $(NH_3H_2O)^+$ and $(NH_3)_2^+$ at the DFT, MP2, and CCSD(T) Levels of Theory[a]

				$(NH_3)_2^+$	
method	scale factor[b]	H_2O	NH_3	$H_3NH^+\cdots NH_2$	$(H_3N\cdots NH_3)^+$
MPW1K/6-311++G**	0.919	3764,3664	3438,3438,3311	3346_{14},3346_{14},3335_4,3254_5,3249_3,2347_{210}	3443_{17},3443_{19},3442_4,3442_7,3295_0,3278_{23}
MP2/aVTZ	0.950	3749,3630	3465,3464,3325	3394_4,3384_{14},3384_{14},3299_1,3280_8,2469_{190}	3476_{17},3476_{17},3474_5,3474_5,3317_0,3314_1
CCSD(T)/aVDZ	0.965	3765,3652	3445,3445,3312	3403,3403,3361,3296,3267,2564	3487,3487,3485,3485,3323,3308

	$(NH_3H_2O)^+$		
method	$H_2NH^+\cdots OH_2$	$H_3N^+\cdots OH_2$	$H_3NH^+\cdots OH$
MPW1K/6-311++G**	3703_{23},3618_{10},3377_{19},3270_{14},2319_{214}	3697_{19},3604_{18},3424_{23},3422_{25},3237_3	3537_{11},3331_{17},3328_{17},3247_{12},2963_{82}
MP2/aVTZ	3697_{20},3597_8,3448_{20},3336_{17},2505_{191}	3692_{16},3588_9,3479_{25},3479_{25},3289_0	3561_{10},3372_{16},3370_{16},3278_{14},2999_{80}
CCSD(T)/aVDZ	3742,3642,3439,3324,2562	3721,3617,3485,3484,3280	3539,3395,3392,3298,3045

[a] The frequencies of NH_3, NH_3^+, H_2O, and H_2O^+ are reported for comparison. [b] See the text.

molecule is more easily ionized than the water molecule, almost a full positive charge in the dimer cations is localized at the ammonia or ammonium moiety, except for the $(H_3N\cdots NH_3)^+$ structure for which the charge of the NH_3 moiety is obviously half of a unit.

The barrier heights for the interconversion between the $L_dH\cdots L'$, $L\cdots L'$, and $LH^+\cdots L_d'$ structures are calculated at the MPW1K/6-311++G** level of theory. The CCSD(T)/aVDZ transition structures are closer to the MPW1K/6-311++G** ones than the MP2/aVDZ ones.[10] For the ammonia dimer cation, the transition state [TS]/fg between (f) $H_3NH^+\cdots NH_2$ and (g) $(H_3N\cdots NH_3)^+$ in Figure 2 is higher in energy by 11.11/15.55 kcal/mol than the minimum-energy structure of (f)/(g) at the MPW1K/6-311++G** level and by 10.43/16.36 kcal/mol at the single-point CCSD(T)/aVDZ// MPW1K/6-311++G** level. This transition barrier is moderate. For the ammonia−water cation, the transition state [TS]/ab between (a) $H_2NH^+\cdots OH_2$ and (b) $H_3N^+\cdots OH_2$ is higher in energy by 6.58/0.33 kcal/mol than (a)/(b) at the MPW1K/6-311++G** level and by 6.16/0.24 kcal/mol at the CCSD(T)/aVDZ//MPW1K/6-311++G** level. This transition barrier is still considered to be not small. The transition state [TS]/bc between (c) $H_3NH^+\cdots OH$ and (b) $H_3N^+\cdots OH_2$ is higher in energy by 23.25/27.99 kcal/mol than (c)/(b) at the MPW1K/6-311++G** level and by 23.93/27.96 kcal/mol at the CCSD(T)/aVDZ//MPW1K/6-311++G** level. This transition barrier is high.

The vibrational frequencies of the neutral water monomer and the water monomer cation were discussed in the previous study.[10] The experimental asymmetric ν_3 and symmetric ν_1 frequencies of the ammonia monomer[34] are known to be 3444 and 3337 cm^{-1}, and those of the ammonia monomer cation[35] are 3388 and 3150 cm^{-1}, showing the red shifts by 56 and 187 cm^{-1}, respectively. This is because the strength of N−H bonds is weakened due to the ionization as compared with the neutral ammonia monomer. The calculated unscaled harmonic frequencies of the ammonia monomer are 3739 and 3601 cm^{-1} at the MPW1K/6-311++G**, 3648 and 3501 cm^{-1} at the MP2/aVTZ, and 3571 and 3434 cm^{-1} at the CCSD(T)/aVDZ level. Those of the ammonia monomer cation are 3634 and 3449 cm^{-1} at the MPW1K/6-311++G**, 3602 and 3411 cm^{-1} at the MP2/aVTZ, and 3542 and 3340 cm^{-1} at the CCSD(T)/aVDZ level. Then, the red shifts are 105 and 152 cm^{-1} at the MPW1K/6-311++G**, 46 and 90 cm^{-1} at the MP2/aVTZ, and 29 and 96 cm^{-1} at the CCSD(T)/aVDZ level. Though the values are based on the harmonic frequencies, the red shifts seem to be better represented at the MPW1K/6-311++G** level than the other methods.

The calculated vibrational frequencies of the water monomer and the ammonia monomer show different deviations from the experimental frequencies. Thus, we used the average scale factor to match both NH_3 and H_2O frequencies properly. The scale factors are 0.919 at the MPW1K/6-311++G**, 0.950 at the MP2/aVTZ, and 0.965 at the CCSD(T)/aVDZ level.

We have calculated the frequencies of the N−H and O−H stretching modes of the ammonia−water cation [(a) $H_2NH^+\cdots OH_2$, (b) $H_3N^+\cdots OH_2$, and (c) $H_3NH^+\cdots OH$] and the ammonia dimer cation [(f) $H_3NH^+\cdots NH_2$ and (g) $(H_3N\cdots NH_3)^+$] at the MPW1K, MP2, and CCSD(T) levels (Figure 3 and Table 7). At the CCSD(T)/aVDZ level, structure (g) $(H_3N\cdots NH_3)^+$ shows six weakly red-shifted N−H stretching frequencies of 3308, 3323, 3485, 3485, 3487, and 3487 cm^{-1}, while structure (f) $H_3NH^+\cdots NH_2$ shows one strongly red-shifted peak and five weakly red-shifted peaks at 2564, 3267, 3296, 3361, 3403, and 3403 cm^{-1}. One strongly red-shifted frequency (2564 cm^{-1} at the CCSD(T)/aVDZ level) for (f) $H_3NH^+\cdots NH_2$ is of the ammonium moiety (H_3NH^+) interacting with the $\bullet NH_2$ radical. In the ammonia−water cation, structure (a) $H_2NH^+\cdots OH_2$ produces a more strongly red-shifted NH stretching frequency (2562 cm^{-1}) than (c) $H_3NH^+\cdots OH$ (3045 cm^{-1}) at the CCSD(T)/aVDZ level. The five weakly red-shifted N−H and O−H stretching modes of structure (b) $H_3N^+\cdots OH_2$ appear at 3280, 3484, 3485, 3617, and 3721 cm^{-1} at the CCSD(T)/aVDZ level of theory.

Concluding Remarks

At the CCSD(T)/CBS level of theory, for $(NH_3\cdots H_2O)^+$, the $H_2NH^+\cdots OH_2$ structure is the lowest, 2 kcal/mol more stable than the $H_3NH^+\cdots OH$ structure and 4 kcal/mol more stable than the $H_3NH^+\cdots OH$ structure. For $(NH_3)_2^+$, the $H_3NH^+\cdots NH_2$ structure is the most stable, 5 kcal/mol more stable than the $(H_3N\cdots NH_3)^+$ structure. On the other hand, most DFT calculations with various functionals predict wrong structures in favor of the $L\cdots L'$ form. Nevertheless, the DFT results with MPW1K and BH&HLYP functionals provide the right structures and energetics, which are very close to the CCSD(T)/CBS results. In this regard, the energy comparison of these structures would be an important criterion for the validity test of the DFT functionals. The MP2 calculations give reasonable energies for most structures but unreasonable frequencies for the $L\cdots L'$ structures. Therefore, in order to obtain reliable stabilities and frequencies, the CCSD(T) calculations were necessary. However, the DFT (MPW1K) is an alternative approach to obtain reasonably reliable results for this system with much less computing time. The calculated spectra are provided to facilitate future experiments.

Acknowledgment. This work was supported by a Korea Research Foundation Grant (KRF-2006-353-C00022) funded by

the Korean Government (MOEHRD). The support from the KISTI Supercomputing Center (KSC-2007-S00-3005) is also acknowledged. H.M.L. thanks Prof. M. Kolaski for discussions.

References and Notes

(1) (a) Chaban, G. M.; Gerber, R. B.; Janda, K. C. *J. Phys. Chem. A* **2000**, *105*, 8323. (b) Re, S.; Osamura, Y.; Suzuki, Y.; Schaefer, H. F., III. *J. Chem. Phys.* **1998**, *109*, 973. (c) Lee, C.; Sosa, C.; Planas, M.; Novoa, J. J. *J. Chem. Phys.* **1996**, *104*, 7081. (d) Smith, A.; Vincent, M. A.; Hillier, I. H. *J. Phys. Chem. A* **1999**, *103*, 1132. (e) Cabaleiro-Lago, E. M.; Hernida-Ramon, J. M.; Rodriguez-Otero, J. *J. Chem. Phys.* **2002**, *117*, 3160. (f) Odde, S.; Pak, C.; Lee, H. M.; Kim, K. S.; Mhin, B. J. *J. Chem. Phys.* **2004**, *121*, 204. (g) Singh, N. J.; Olleta, A. C.; Kumar, A.; Park, M.; Yi, H.-B.; Bandyopadhyay, I.; Lee, H. M.; Tarakeshwar, P.; Kim, K. S. *Theor. Chem. Acc.* **2006**, *115*, 127. (h) Robertson, W. H.; Johnson, M. A. *Science* **2002**, *298*, 4.

(2) (a) Kumar, A.; Park, M.; Huh, J. Y.; Lee, H. M.; Kim, K. S. *J. Phys. Chem. A* **2006**, *110*, 12484. (b) Veerman, A.; Lee, H. M.; Kim, K. S. *J. Chem. Phys.* **2005**, *123*, 084321. (c) Odde, S.; Lee, H. M.; Kolaski, M.; Mhin, B. J.; Kim, K. S. *J. Chem. Phys.* **2004**, *121*, 4665.

(3) (a) Godinho, S. S. M. C.; do Couto, P. C.; Cabral, B. J. C. *J. Chem. Phys.* **2005**, *122*, 044316. (b) Olleta, A. C.; Lee, H. M.; Kim, K. S. *J. Chem. Phys.* **2006**, *124*, 024321. (c) Olleta, A. C.; Lee, H. M.; Kim, K. S. *J. Chem. Phys.* **2007**, *126*, 144311. (d) Pye, C. C.; Tomney, M. R.; Enright, T. G. *Can. J. Anal. Sci. Spectrosc.* **2005**, *50*, 254. (e) Singh, N. J.; Yi, H.-B.; Min, S. K.; Park, M.; Kim, K. S. *J. Phys. Chem. B* **2006**, *110*, 3808. (f) Park, J. M.; Cho, J.-H.; Kim, K. S. *Phys. Rev. B* **2004**, *69*, 233403.

(4) (a) Shinohara, H.; Nishi, N.; Washida, N. *J. Chem. Phys.* **1986**, *84*, 5561. (b) de Visser, S. P.; de Koning, L. J.; Nibbering, N. M. M. *J. Phys. Chem.* **1995**, *99*, 15444. (c) Jongma, R. T.; Huang, Y.; Shi, S.; Wodtke, A. M. *J. Phys. Chem. A* **1998**, *102*, 8847. (d) Angel, L.; Stace, A. J. *Chem. Phys. Lett.* **2001**, *345*, 277.

(5) (a) Barnett, R. N.; Landman, U. *J. Phys. Chem.* **1995**, *99*, 17305. (b) Barnett, R. N.; Landman, U. *J. Phys. Chem. A* **1997**, *101*, 164.

(6) (a) Novakovskaya, Y. V.; Stepanov, N. F. *J. Phys. Chem. A* **1999**, *103*, 3285. (b) Gill, P. M. W.; Radom, L. *J. Am. Chem. Soc.* **1988**, *110*, 4931.

(7) (a) Sodupe, M.; Bertran, J.; Rodriguez-Santiago, L.; Baerends, E. J. *J. Phys. Chem. A* **1999**, *103*, 166. (b) Grning, M.; Gritsenko, O. V.; van Gisbergen, S. J. A.; Baerends, E. J. *J. Phys. Chem. A* **2001**, *105*, 9211.

(8) (a) Muller, I. B.; Cederbaum, L. S. *J. Chem. Phys.* **2006**, *125*, 204305. (b) Tachikawa, H. *J. Phys. Chem. A* **2004**, *108*, 7853.

(9) (a) Tomoda, S.; Kimura, K. *Chem. Phys. Lett.* **1985**, *121*, 159. (b) Azeim, S. A.; van der Rest, G. *J. Phys. Chem. A* **2005**, *109*, 2505.

(10) Lee, H. M.; Kim, K. S. *J. Chem. Theory Comput.* **2009**, *5*, 976.

(11) (a) Pribble, R. N.; Zwier, T. S. *Science* **1994**, *265*, 75. (b) Kim, K. S.; Mhin, B. J.; Choi, U.-S.; Lee, K. *J. Chem. Phys.* **1992**, *97*, 6649. (c) Kim, J.; Kim, K. S. *J. Chem. Phys.* **1998**, *109*, 5886. (d) Xantheas, S. S.; Dunning, T. H. *J. Phys. Chem.* **1992**, *96*, 7505. (e) Lee, H. M.; Suh, S. B.; Lee, J. Y.; Tarakeshwar, P.; Kim, K. S. *J. Chem. Phys.* **2000**, *112*, 9759. (f) Buck, U.; Huisken, F. *Chem. Rev.* **2000**, *100*, 3863.

(12) (a) Pak, C.; Lee, H. M.; Kim, J. C.; Kim, D.; Kim, K. S. *Struct. Chem.* **2005**, *16*, 187. (b) Liu, S.-Y.; Dykstra, C. E.; Kolenbrander, K.; Lisy, J. M. *J. Chem. Phys.* **1986**, *85*, 2077. (c) Jeffrey, G. A. *An Introduction to Hydrogen Bonding*; Truhlar, D., Ed; Oxford University Press: New York, 1997.

(13) (a) Becke, A. D. *Phys. Rev A* **1988**, *38*, 3098. (b) Lee, C.; Yang, W.; Parr, R. G. *Phys. Rev. B* **1988**, *37*, 785.

(14) Perdew, J. P.; Burke, K.; Wang, Y. *Phys. Rev. B* **1996**, *54*, 16533.

(15) Boese, A. D.; Handy, N. C. *J. Chem. Phys.* **2001**, *114*, 5497.

(16) (a) Slater, J. C. *Quantum Theory of Molecular and Solids*; McGraw-Hill: New York, 1974; Vol. 4. (b) Vosko, S. H.; Wilk, L.; Nusair, M. *Can. J. Phys.* **1980**, *58*, 1200.

(17) Grimme, S. *J. Comput. Chem.* **2006**, *27*, 1787.

(18) Tao, J. M.; Perdew, J. P.; Staroverov, V. N.; Scuseria, G. E. *Phys. Rev. Lett.* **2003**, *91*, 146401.

(19) Becke, A. D. *J. Chem. Phys.* **1993**, *98*, 5648.

(20) Zhao, Y.; Schultz, N. E.; Truhlar, D. G. *J. Chem. Theory Comput.* **2006**, *2*, 364.

(21) Perdew, J. P.; Burke, K.; Ernzerhof, M. *Phys. Rev. Lett.* **1997**, *78*, 1396.

(22) Lynch, B. J.; Fast, P. L.; Harris, M.; Truhlar, D. G. *J. Phys. Chem. A* **2000**, *104*, 4811.

(23) Zhao, Y.; Truhlar, D. G. *J. Phys. Chem. A* **2004**, *108*, 6908.

(24) Note that BH&H means the $0.5E_X^{HF} + 0.5E_X^{LSDA} + E_C^{LYP}$ functional.

(25) Note that BH&HLYP means the $0.5E_X^{HF} + 0.5E_X^{LSDA} + 0.5\Delta E_X^{Becke88} + E_C^{LYP}$functional.

(26) Krishnan, R.; Binkley, J. S.; Seeger, R.; Pople, J. A. *J. Chem. Phys.* **1980**, *72*, 650.

(27) Dunning, T. H., Jr. *J. Chem. Phys.* **1989**, *90*, 1007.

(28) (a) Helgaker, T.; Ruden, T. A.; Jorgensen, P.; Olsen, J.; Klopper, W. *J. Phys. Org. Chem.* **2004**, *17*, 913. (b) Min, S. K.; Lee, E. C.; Lee, H. M.; Kim, D. Y.; Kim, D.; Kim, K. S. *J. Comput. Chem.* **2008**, *29*, 1208. (c) Lee, E. C.; Kim, D.; Jurecka, P.; Tarakeshwar, P.; Hobza, P.; Kim, K. S. *J. Phys. Chem. A* **2007**, *111*, 3446.

(29) Frisch, M. J.; Trucks, G. W.; Schlegel, H. B.; Scuseria, G. E.; Robb, M. A.; Cheeseman, J. R.; Zakrzewski, V. G.; Montgomery, J. A., Jr.; Stratmann, R. E.; Burant, J. C.; Dapprich, S.; Millam, J. M.; Daniels, A. D.; Kudin, K. N.; Strain, M. C.; Farkas, O.; Tomasi, J.; Barone, V.; Cossi, M.; Cammi, R.; Mennucci, B.; Pomelli, C.; Adamo, C.; Clifford, S.; Ochterski, J.; Petersson, G. A.; Ayala, P. Y.; Cui, Q.; Morokuma, K.; Salvador, P.; Dannenberg, J. J.; Malick, D. K.; Rabuck, A. D.; Raghavachari, K.; Foresman, J. B.; Cioslowski, J.; Ortiz, J. V.; Baboul, A. G.; Stefanov, B. B.; Liu, G.; Liashenko, A.; Piskorz, P.; Komaromi, I.; Gomperts, R.; Martin, R. L.; Fox, D. J.; Keith, T.; Al-Laham, M. A.; Peng, C. Y.; Nanayakkara, A.; Challacombe, M.; Gill, P. M. W.; Johnson, B.; Chen, W.; Wong, M. W.; Andres, J. L.; Gonzalez, C.; Head-Gordon, M.; Replogle, E. S.; Pople, J. A. *Gaussian 03*, revision A.1; Gaussian, Inc.: Pittsburgh, PA, 2003.

(30) (a) Neese, F. *J. Chem. Phys.* **2001**, *115*, 11080. (b) Neese, F. *ORCA - an Ab Initio, DFT and Semiempirical Program Package*, Version 2.6.63; Institute for Physical and Theoretical Chemistry: Bonn, Germany, 2007.

(31) Shao, Y.; Fusti-Molnar, L.; Jung, Y.; Kussmann, J.; Ochsenfeld, C.; Brown, S. T.; Gilbert, A. T. B.; Slipchenko, L. V.; Levchenko, S. V.; O'Neill, D. P.; Distasio, R. A.; Lochan, R. C.; Wang, T.; Beran, G. J. O.; Besley, N. A.; Herbert, J. M.; Lin, C. Y.; Van Voorhis, T.; Chien, S. H.; Sodt, A.; Steele, R. P.; Rassolov, V. A.; Maslen, P. E.; Korambath, P. P.; Adamson, R. D.; Austin, B.; Baker, J.; Byrd, E. F. C.; Daschel, H.; Doerksen, R. J.; Dreuw, A.; Dunietz, B. D.; Dutoi, A. D.; Furlani, T. R.; Gwaltney, S. R.; Heyden, A.; Hirata, S.; Hsu, C.-P.; Kedziora, G.; Khalliulin, R. Z.; Klunzinger, P.; Lee, A. M.; Lee, M. S.; Liang, W.; Lotan, I.; Nair, N.; Peters, B.; Proynov, E. I.; Pieniazek, P. A.; Rhee, Y. M.; Ritchie, J.; Rosta, E.; Sherrill, D. C.; Simmonett, A. C.; Subotnik, J. E.; Woodcock, H. L.; Zhang, W.; Bell, A. T.; Chakraborty, A. K.; Chipman, D. M.; Keil, F. J.; Warshel, A.; Hehre, W. J.; Schaefer, H. F.; Kong, J.; Krylov, A. I.; Gill, P. M. W.; Head-Gordon, M. *Q-Chem*, Version 3.2 (test version); Q-Chem, Inc.: Pittsburgh, PA, 2006.

(32) Lee, S. J.; Chung, H. Y.; Kim, K. S. *Bull. Korean Chem. Soc.* **2004**, *25*, 1061.

(33) (a) Rosenstock, H. M.; Draxl, K.; Steiner, B. W.; Herron, J. T. *J. Phys. Chem. Ref. Data 6* **1977**, *70* (Suppl. 1), 218. (b) Edvardsson, D.; Baltzer, P.; Karlsson, L.; Wannberg, B.; Holland, D. M. P.; Shaw, D. A.; Rennie, E. E. *J. Phys. B: At. Mol. Opt. Phys.* **1999**, *32*, 2583.

(34) (a) Ribbegard, G. *Chem. Phys. Lett.* **1974**, *25*, 333. (b) Coy, S. L.; Lehmann, K. K. *Spectrochim. Acta* **1989**, *45A*, 47.

(35) (a) Agren, H.; Reineck, I.; Veenhuizen, H.; Maripuu, R.; Arneberg, R.; Karlson, L. *Mol. Phys.* **1982**, *45*, 477. (b) Bawendi, M. G.; Rehfuss, B. D.; Dinelli, B. M.; Okumura, M.; Oka, T. *J. Chem. Phys.* **1989**, *90*, 5910.

JP903093A